Geofísica Internacional (2004), Vol. 43, Num. 1, pp. 29-39

Observations of atmospheric gravity waves using airglow all-sky CCD imager at Cachoeira Paulista, Brazil (23° S, 45° W)

A. F. Medeiros[1], H. Takahashi[2], P. P. Batista[2], D. Gobbi[2] and M. J. Taylor[3]

[1] *Universidade Federal Campina Grande (UFCG), Bodocongó, Campina Grande, Paraíba, Brasil*

[2] *Instituto Nacional de Pesquisas Espaciais (INPE), São José dos Campos, São Paulo, Brasil*

[3] *Space Dynamics Laboratory and Physics Department, Utah State University, Utah, USA*

Received: March 31, 2002; accepted: July 29, 2002

RESUMEN

Un fotómetro imageador CCD all-sky fue operado en Cachoeira Paulista (CP), Brasil (23° S, 45° O), con la colaboración de la Utah State University – EUA, durante 12 meses para la observación de las emisiones de aeroluminiscencia en OH, O_2 y OI (557.7 nm). De estas observaciones fueron retiradas las componentes dominantes de las ondas de gravedad e investigadas sus variaciones con las estaciones del año. Estas ondas tienen típicamente longitud de onda horizontal corta (5 – 60 km), período corto (5 – 35 minutes) y velocidad de fase horizontal entre 1 y 80 m/s. Las ondas del tipo banda (longitud de onda horizontal entre 10 y 60 km), muestran una clara dependencia en su dirección de propagación horizontal, moviéndose para el sudeste en el verano y para el noroeste en el invierno. La dirección de propagación cambia a mediados del mes de marzo y al final de septiembre. Nuestros resultados sugieren que las ondas de gravedad en CP son generadas por una fuerte convección troposférica. En el verano esta región se extiende en una linea entre los 10° S, 45° O y 40° S, 78° O cubriendo desde la parte septentrional de la Argentina al nordeste del Brasil, teniendo una acentuada distribuición en la parte central brasileña y siendo que CP está abajo de esta región. En el invierno y en contraste con el verano, la región convectiva se localiza abajo de CP, principalmente sobre el mar, sin esta convección en la región central del Brasil, arriba de CP. La conclusión más importante es que la anisotropía en la dirección de propagación de las ondas se debe principalmente a la localización de la fuente y su filtraje por los vientos estratosféricos.

PALABRAS CLAVE: Ondas de gravedad, resplandor atmosférico, imageador, diagrama de bloques, vientos.

ABSTRACT

An all-sky CCD imager for OH, O_2 and OI (557.7 nm) airglow was operated at Cachoeira Paulista (CP), Brazil, (23° S, 45° W), from October 1998 to September 1999, with Utah State University. Dominant gravity wave components are extracted and seasonal variations are investigated. These waves have typically short horizontal wavelengths (5 – 60 km), short periods (5 – 35 minutes), and horizontal phase speeds of 1 – 80 m/s. Band-type waves of horizontal wavelength between 10 and 60 km showed clear seasonal dependence in the horizontal propagation direction to southeast in summer and to northwest in winter. The direction of propagation changed in mid-March and at the end of September. The gravity waves over CP may be generated by the strong tropospheric convection. In summer, this region extends along a line approximately between (10° S, 45° W) and (40° S, 78° W), from northern Argentina to the Brazilian northeast, with an accentuated distribution over central Brazil. CP is below this region. In winter, the convective region is located below CP mainly over the sea and there is no convection in central Brazil region above CP. Thus the anisotropy of the wave propagation direction is mainly due to source location and wave filtering by stratospheric winds.

KEY WORDS: gravity waves, airglow, imager, blocking diagram, winds.

1. INTRODUCTION

Over the past few decades much research has been done to understand the role of atmospheric small scale dynamics, such as internal buoyancy waves, in the global circulation system of the atmosphere. An internal buoyancy wave, or gravity wave, is the result of a perturbation of the stable atmosphere in which gravity and buoyancy act as restoring forces. The impact caused by gravity waves is a significant deviation of the general circulation from radiative equilibrium.

Since internal atmospheric gravity waves were recognized as an important atmospheric phenomenon (Hines, 1960), considerable observational and theoretical research has been carried out. These efforts have established the importance of such motions as a part of the driving force of the mean circulation and thermal structure of the Mesosphere and Lower Thermosphere (MLT) region via wave energy and momentum transports (Fritts, 1993).

Considerable progress has been made in observational techniques of gravity waves in the MLT. Some of these techniques are MF radar (Vincent and Fritts, 1987; Manson *et al*., 1997; Thayaparan ,1997; Fritts *et al.* ,1998); incoherent scattering radar (Burnside *et al*.,1991; Rishbeth and Vaneyken,1993; Kirchengast *et al*.,1996; Oliver *et al*., 1997); MST radar (Riggin *et al*. 1995); MU radar (Takahashi *et*

al.,1998,1999); lidar (Clemesha,1995; Clemesha *et al.*,1999, Gardner *et al.*, 1995, Bills and Gardner,1993; She *et al.*,1991); photometer (Takahashi *et al.*,1974; Buriti, 1997); photographic camera (Peterson and Keiffaber 1973, Moreels and Herse,1977; Herse *et al.*, 1980); television camera (Hapgood and Taylor,1982; Taylor and Edwards,1991); imager with CCD(Taylor *et al*,1995a; Taylor and Garcia, 1995; Garcia and Taylor,1997; Hecht *et al.* ,1994; Swenson and Mende,1994); Fabry-Perot interferometer (Hernandez *et al.*,1993) and Michelson interferometer (Lowe and Turnbull,1995; Sivjee and Walterscheid,1994; Gault *et al.*,1996; Shepherd,1996).

Airglow imaging techniques provide a simple and useful method for investigating the horizontal characteristics of the gravity waves and their temporal evolution at MLT heights. Most of the airglow image measurements reported in the literature concern to short-period (<1 hour) wave structures and they fall into two distinct categories called "bands" and "ripples". Bands are extensive, long-lasting wave patterns which exhibit horizontal wavelengths of several tens of kilometers and horizontal phase velocities up to 100 m/s (e.g. Clairemidi *et al.*, 1985). These patterns have been attributed to freely propagating or ducted short-period gravity waves (Walterscheid *et al.*, 1999; Isler *et al.*, 1997; Taylor *et al.*, 1987). Ripples are short-lived (<45 min) small-scale wave patterns of restricted spatial extent (Peterson, 1979), and are thought to be generated *in situ* by localized shear or convective-type instabilities in the total wind field (Taylor and Hapgood, 1990; Hecht *et al.*, 1995).

Nakamura *et al.* (1999) analyzed 18 months of observation in the OH images, extracted dominant gravity wave component and investigated seasonal variation of the characteristics of the waves. Walterscheid *et al.* (1999) analyzing 9 months of airglow image observations of atmospheric gravity waves proposed that many waves were thermally ducted. Hecht *et al.* (2001) analyzing 15 months of observations suggested that the waves originated no more than a few thousand kilometers from the observation site. This paper describes new image measurements of short period waves observed from a low-latitude site in the Southern Hemisphere.

The main goal of this paper was to construct a seasonal variation behaviour of the short period gravity waves over CP using an all-sky airglow imager. Maybe the most important result of this work has been the appearance of an anisotropy in the propagation direction of the observed waves. After reaching this objective, one second objective, not less important, was to understand the causes of the observed features. For explaining these features, we discuss the data using the filtering wave theory and searched for likely generating sources of the waves. The result was that the waves over CP are generated by strong convective regions and that anisotropy in propagation direction are in part due to the location (seasonal variation) of the generating sources and mainly to the filtering of the waves by stratospheric winds.

2. INSTRUMENTATION AND METHODOLOGY

Routine airglow observations have been carried out at CP using an all-sky imaging system. This is a collaborative program between the Instituto Nacional de Pesquisas Espaciais (INPE), Brazil and the Space Dynamics Laboratory, Utah State University (Dr. M. J. Taylor). The CCD imager consists of a large area (6.45 cm^2), high resolution, 1024x1024 back-illuminated array with a pixel size of 14 bits. The high quantum efficiency (~80% at visible wavelengths), low dark current (0.5 electrons/pixel/s), low readout noise (15 electrons rms), and high linearity (0.05%) of this device made it possible to achieve quantitative measurements of the airglow emissions. The camera uses a fast (f/4) all-sky telecentric lens system that enables high signal-to-noise (20:1) images of wave structure to be obtained with time integration of typically 15 s for the near-infrared OH emission (715-930 nm pass-band) and 90 s for the OI, O_2, and OI(630.0 nm) emissions. The image was binned on-chip down to 512x512 resolution to enhance the signal-to-noise ratio.

For the large-field information present in the all-sky data, accurate spatial calibration is essential. We can achieve this by using the stars in each image as known reference points in the sky. We determine the lens function by performing a least-square fit using the measured position of the stars in the original image. After we have processed the all-sky images, it is now possible to determine the horizontal wave parameters directly with standard 2-D FFT analysis. The advantage of this method is that measurements of all of the monochromatic features present in the data are now possible.

We can investigate gravity wave content in any part of the image by isolating the region of interest, taking the 2-D FFT of the selected region and investigating peaks in the frequency spectrum. Other way to show these events is to show in three dimensions.

The determination of the period (and hence phase speed) of the waves present in these data involves taking the one-dimensional (1-D) FFT in the time of the complex 2-D FFT in space. The peaks in the 1-D FFT correspond to the wave frequencies present in the data.

3. RESULTS

The imaging system was located at CP (23° S, 45° W). Measurements were taken from October 1998 to September

1999. This result is depicted in the Figure 1 which plots the frequency of occurrence of the waves. Despite the sometimes severe restrictions imposed by meteorological clouds, approximately 433 hours of useful data were recorded on 69 nights, in which 283 wave events were detected. The mean rate of the events was 0.7 events/hour, with higher mean rate on summer and winter months and lower mean rate on equinoctial months.

The Figures 2 show examples of the gravity waves imaged during the observation period. In the Figure 2 two images showing gravity waves recorded in the OI(557.7 nm) and near-infrared OH emissions with bands (left) and ripples(right).

3.1 Band-Ripple comparison

Of the total 283 wave events, 64% were bands, while 36% were ripples.

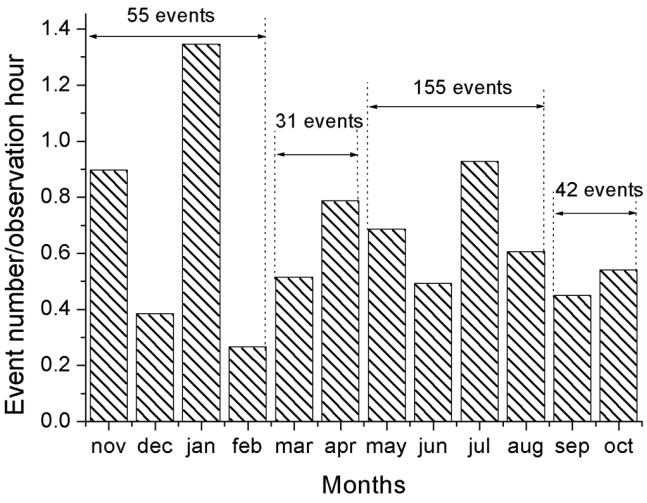

Fig. 1. Frequency of occurrence of waves (ripples and bands) for months.

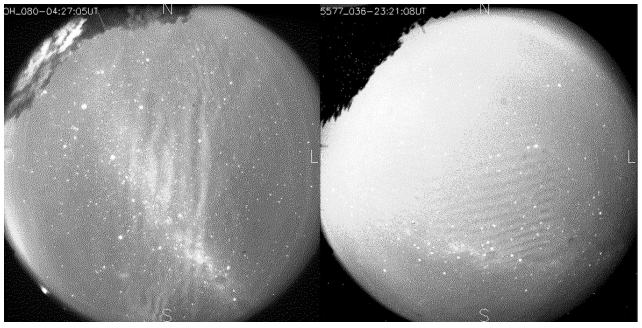

Fig. 2. Gravity waves imaged during observation period. OI(5577 nm) image(right) and OH image(left).

The data have been binned into histograms of 5 km width. This shows the most frequently observed horizontal scale sizes. The strong tendency for ripples to occur over narrow wavelength range is apparent with ~83% of all events having wavelengths in the 10-15 km range. In contrary, the band distribution exhibited a significantly broader range of horizontal wavelengths extending from ~10-60 km and 85% of all bands had wavelengths > 15 km. The average band wavelength was 22.92 km, approximately twice of that for the ripples (12.94 km).

The distribution of observed waves periods have binned at 2 min intervals 5. The ripples exhibit a remarkable sharp distribution centered on the 6-10 min (with 70% of events occurring within this range) and an average wave period of 8.36 min. In comparison, the distribution of the periods of the bands is considerably broader than for the ripples and shows a clear tendency toward longer wave period (with 97% of bands exhibiting periods > 8 min). The bands exhibited an average wave period of 15.62 min.

The distribution of wave phase speeds have plotted at 10 m/s intervals. The bands measurements range from 10 to 80 m/s and exhibit an average value of 26.1 m/s. There is a clear tendency for many of the waves to exhibit phase speed in the 10 40 m/s range. The ripples exhibited a distribution in the range of the 10-60 m/s. The average phase speed was of 27.2 m/s.

The last parameter analyzed was the wave propagation direction. The propagation direction for both groups, binned over 15° intervals, are plotted in Figure 3 The distribution of bands (Figure 3a) is highly anisotropic. There are two directions of preference: southeast (azimuth range 90°-180°) and northwest (azimuth range 270°-360°). The ripples (Figure 3b) presented propagation direction in all azimuths and did not show a preferential direction.

3.2 Band-Ripple seasonal variation

After the general comparison of the bands and ripples, we analyzed the parameters (wavelength, period, phase velocity and propagation direction) distributed for each group by each season. The total observation period was separated in four seasons: summer (November, December, January and February), autumn (March and April), winter (May, June, July and August) and spring (September and October).

This analysis did not show a clear seasonal variation for wavelengths, periods and phase velocities, neither for ripples or bands. The ripples also did not present seasonal variation for propagation direction. However, the bands showed an evident seasonal variation for propagation direction. The Figure 4 shows a clear preference of the bands for

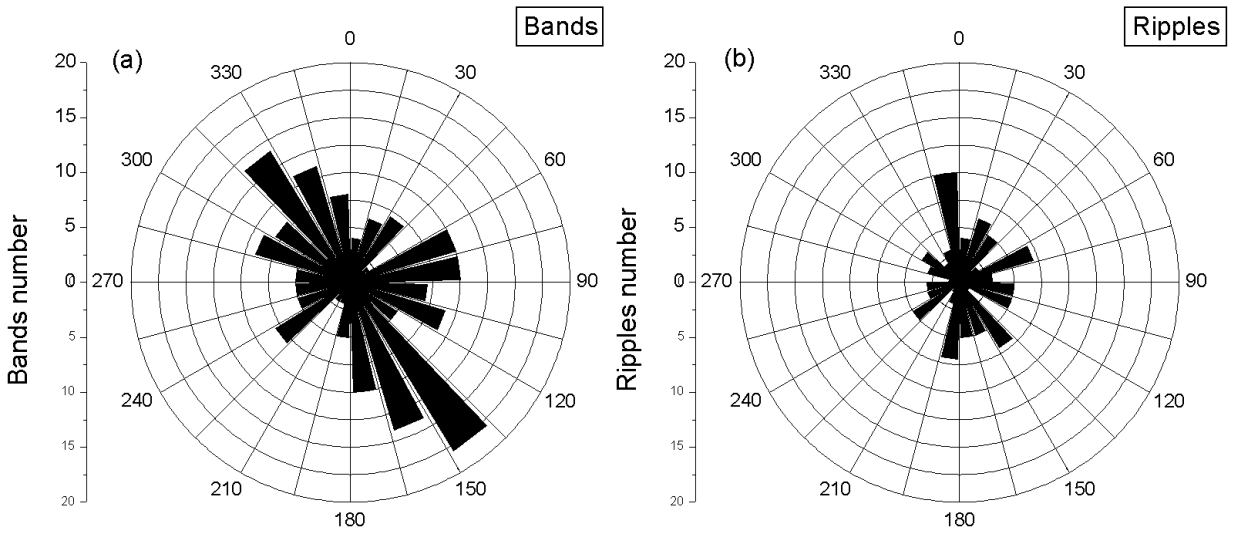

Fig. 3. Polar histogram of the propagation direction for bands(a) and ripples(b) binned over 15° intervals.

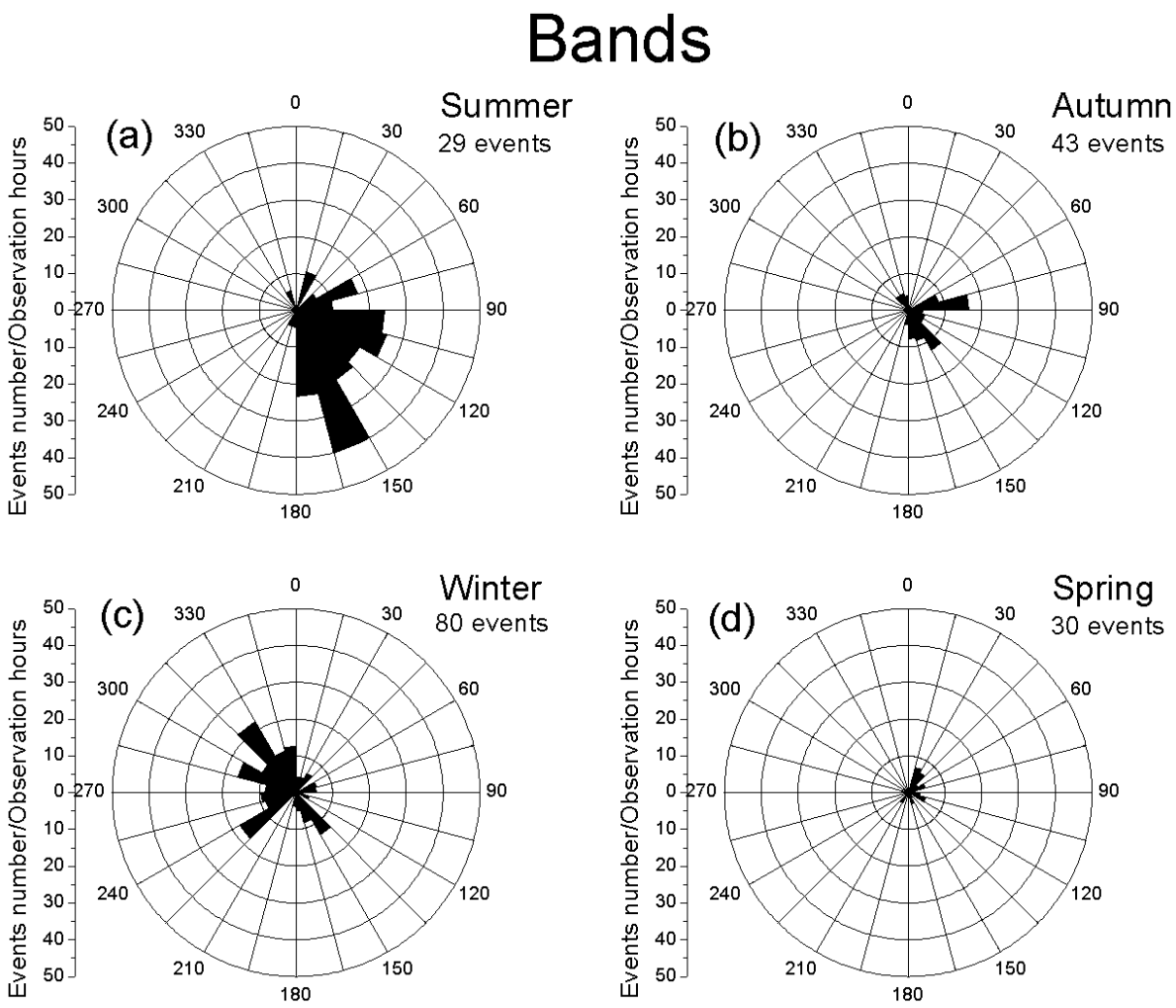

Fig. 4. Polar histograms of the propagation direction for bands for each season. Summer (a), Autumn(b), winter(c) and spring(d).

propagation direction in summer and winter. In summer the preferential propagation direction is towards southeast (Figure 4a). In winter the preferential propagation direction is towards northwest (Figure 4c). In the other seasons no clear preferential propagation direction were observed.

4. DISCUSSION

4.1 Preferential direction and filtering

The anisotropy detected in propagation direction of the bands, mainly for summer and winter can be due the presence of critic levels. Gravity waves propagating upward from the lower atmosphere are absorbed into the mean flow as they approach a critical layer where the intrinsic frequency of the wave is Doppler shifted to zero. This situation may occur at any height level when the local horizontal wind speed along the direction of propagation equals the observed horizontal phase speed of the gravity wave.

The Equation 1 was used to determine the forbidden regions (velocities) defined by the regions where the wave frequency $\Omega \leq 0$ at any height below the peak of the layer emissions (OI5577, OH and O_2):

$$v_x = V_z \cos\phi + V_m sen\phi \ , \qquad (1)$$

where V_z is the zonal wind, V_m is the meridional wind and ϕ is the angle between wave vector and east.

Blocking diagrams (Ryan,1991; Ryan and Tuan,1991; Taylor,1993) were plotted for each month of the year using the wind profiles derived from HWM93 (Hedin,1996) for CP. The Figures 5, 6 and 7 show blocking diagrams superimposed with the bands observed for each season of the year and each emission. The results agree in part with the anisotropy detected in the bands. This suggests that the wave filtering by winds can play an important role in the seasonal variation of the waves over CP but it is not the only factor.

4.2 Likely sources

Any perturbation with temporal scales between a few and several minutes that introduces changes in the atmosphere

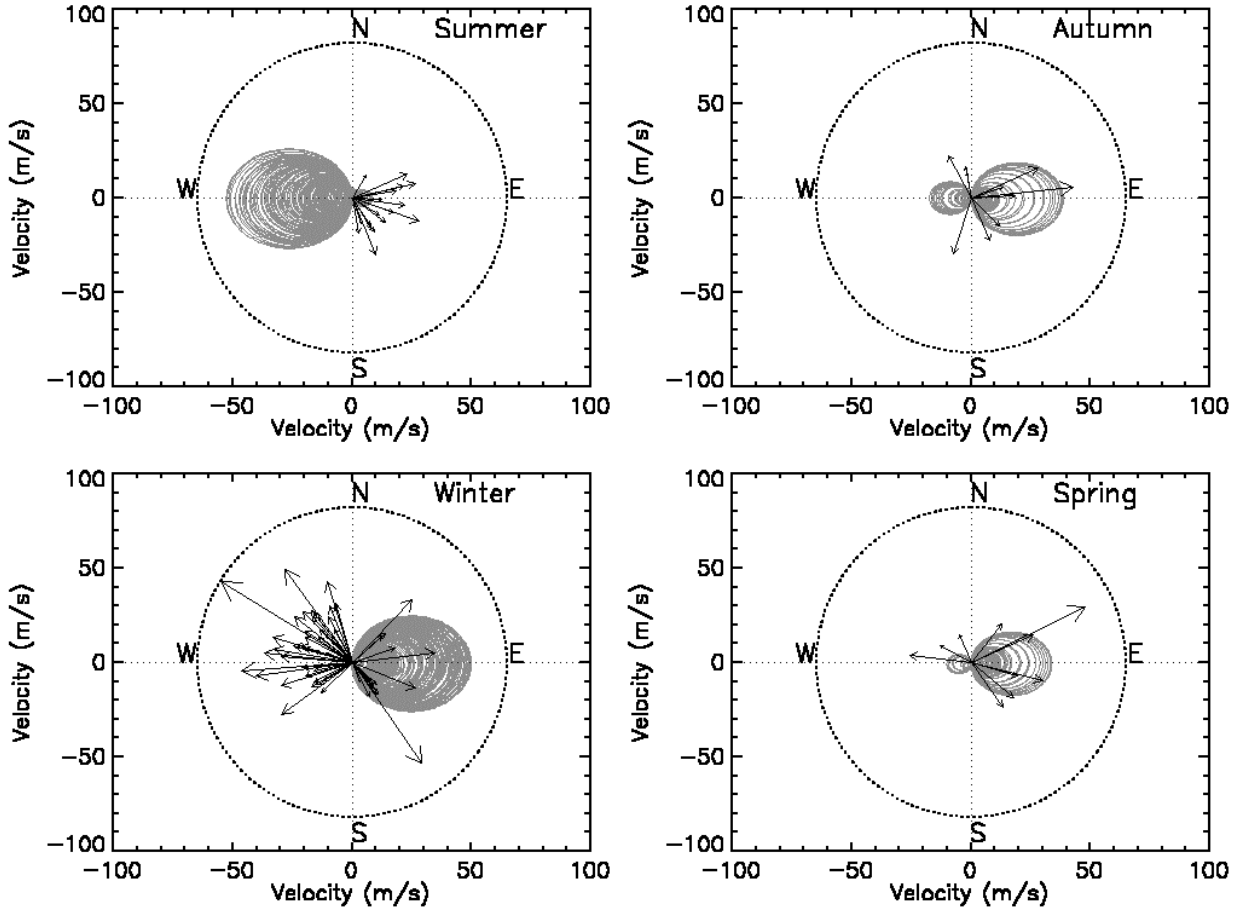

Fig. 5. Blocking diagrams superimposed with the bands observed from each season of the year for bands detected in OH layer.

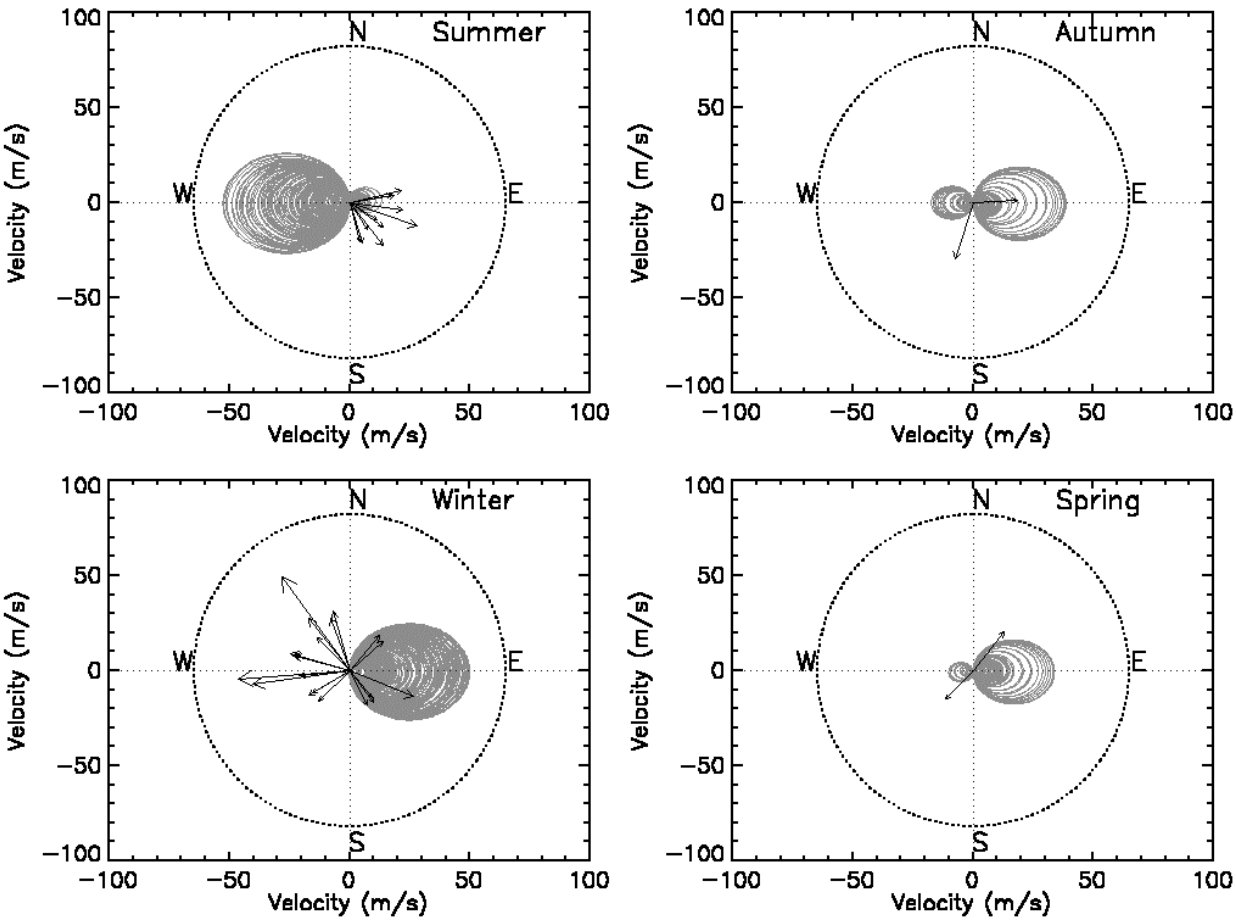

Fig. 6. Blocking diagrams superimposed with the bands observed for each season of the year for bands detected in O_2 layer.

may generate gravity waves. Nowadays the tropospheric sources are thought as possible generators of the waves in all latitudes (Taylor, 1988).

In this work we used airglow image data together with satellite image (GOES8) data and Lightning imaging sensor (LIS) data to identify the sources. The LIS is a space based instrument used to detect the distribution and variability of total lightning (cloud-to-cloud, intracloud, and cloud-to-ground lightning) that occurs in the tropical regions of the globe. The LIS is a scientific instrument aboard the TRMM (Tropical Rainfall Measuring Mission) observatory.

The satellite images were used to detect convective regions over South America (area with approximately 1000 km of radius with center in CP).

The LIS data were used for identification of the thunderstorms and to infer seasonal distribution of the lighting over South America. These data also permitted to discuss the anisotropy of the direction of propagation.

Figure 8 shows the lightning distribution in the tropics for summer. Note clearly that most of the lightning occurrence over South America extends approximately in the line from northern Argentina to almost the Brazilian northeast with a conspicuous distribution over central Brazil. CP is located bellow this line, this suggests this convection line as responsible for most of waves over CP directed to southeast in summer.

Figure 9 shows the lightning distribution over the tropics for winter detected by LIS. In contrast with summer the lightning distribution occur bellow CP, mainly over the sea and there is no convection above in central region of the Brazil. This suggests that is this region that contribute for that waves to have propagation direction for northwest in winter.

The analysis of the Figures 8 and 9 and its comparison with the Figures 5, 6 and 7 suggests that gravity waves over CP are generated by strong convection regions (above CP in summer and bellow of CP in winter). This way, the anisotropy of propagation direction is due in part to the location

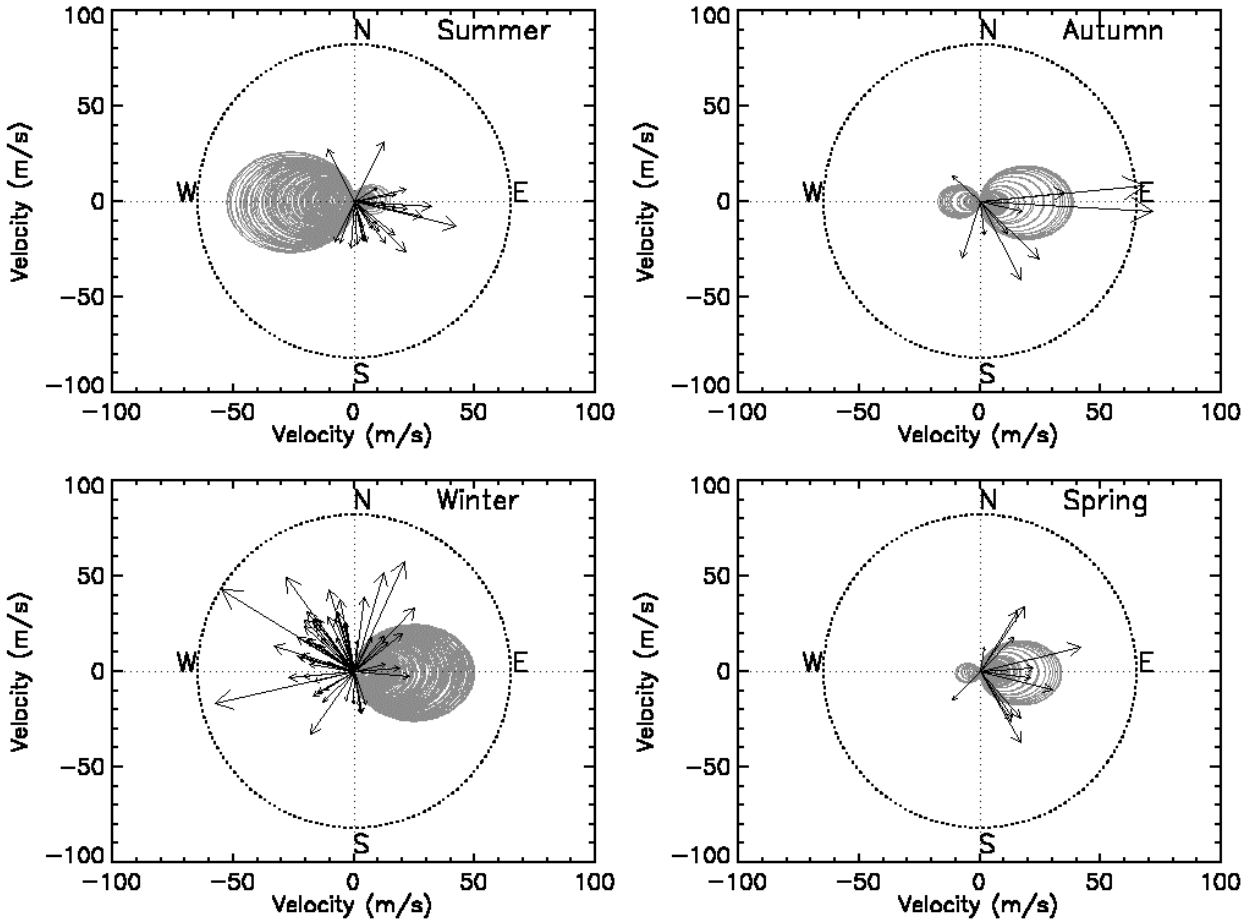

Fig. 7. Blocking diagrams superimposed with the bands observed from each season of the year for bands detected in OI(5577 nm) layer.

of the generating sources and mainly to wave filtering by stratospheric winds.

5. CONCLUSIONS

The present work showed relevant result of the gravity wave observations by the airglow imaging technique carried out at CP (23° S, 45° W) in the period of October 1998 to September 1999. A total of the 69 nights, corresponding to 433 hours of the observations, was analyzed. During the period, 283 wave events were detected in OH, O_2 and OI5577 images. The main results are listed below:

1. Most of wave activity occurred in months of January and February. The events mean rate was 0.7 events/hours, with larger rates in summer and winter months and smaller rates in equinoctial months.
2. Of a total of 283 wave events 64% were classified as bands and 36% as ripples.
3. 83% of the ripples presented wavelength between 10 and 15 km.
4. 85% of the bands presented wavelength larger than 15 km.
5. The mean wavelength for the bands was 22.9 km and for ripples was 12.9 km.
6. 70% of the ripples presented observed periods between 6 and 10 minutes.
7. 97% of the bands displayed observed periods greater than 8 minutes.
8. The ripples displayed an observed mean period of 8.4 minutes, while the bands presented an observed mean period of 15.62 minutes. This corresponds to almost twice the mean period of the ripples.
9. The bands and ripples displayed a similar tendency (between 10 and 40 m/s) for phase velocity.
10. The mean phase velocity for bands was of 26.08 m/s and for ripples was of 27.17 m/s.
11. The wavelengths for the bands have broader distribution (10-60 m/s) in summer and winter.
12. The ripples did not display clear seasonal variation for wavelengths.
13. The bands displayed the same distribution for the observed periods for the four seasons. However, 80% the

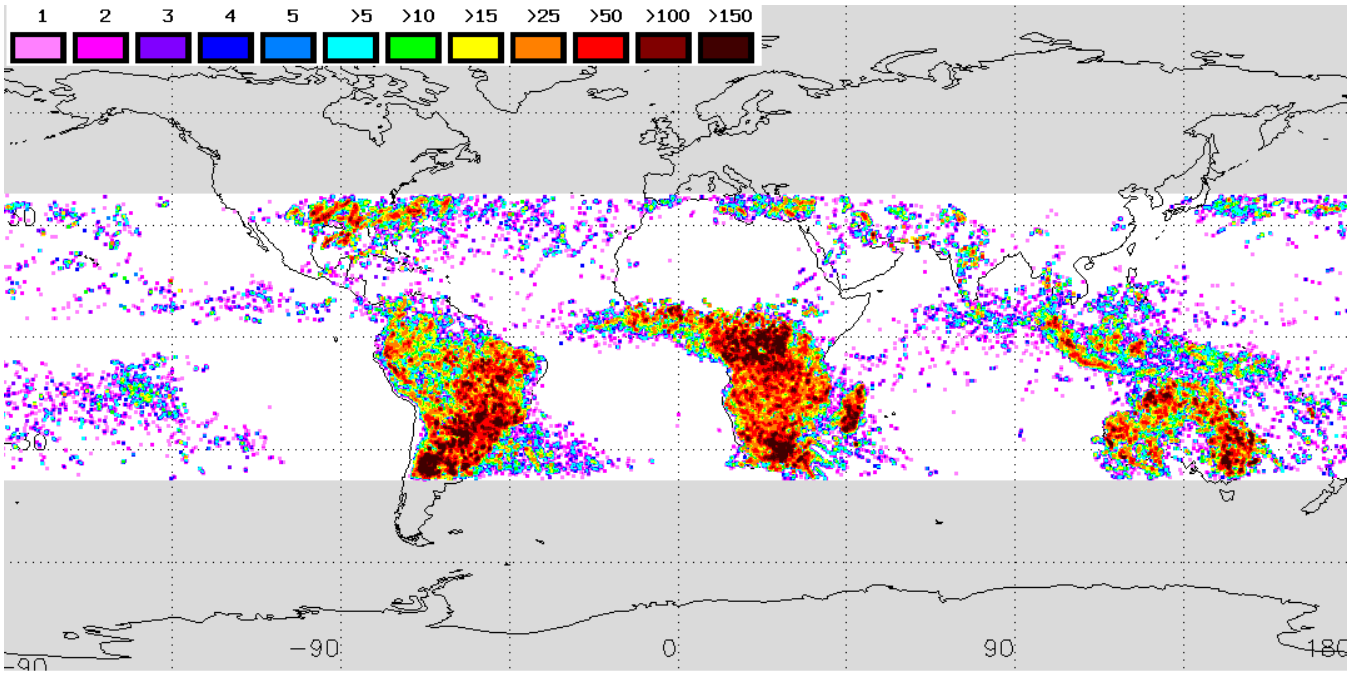

Fig. 8. Lightning distribution in the tropics for summer from LIS data.

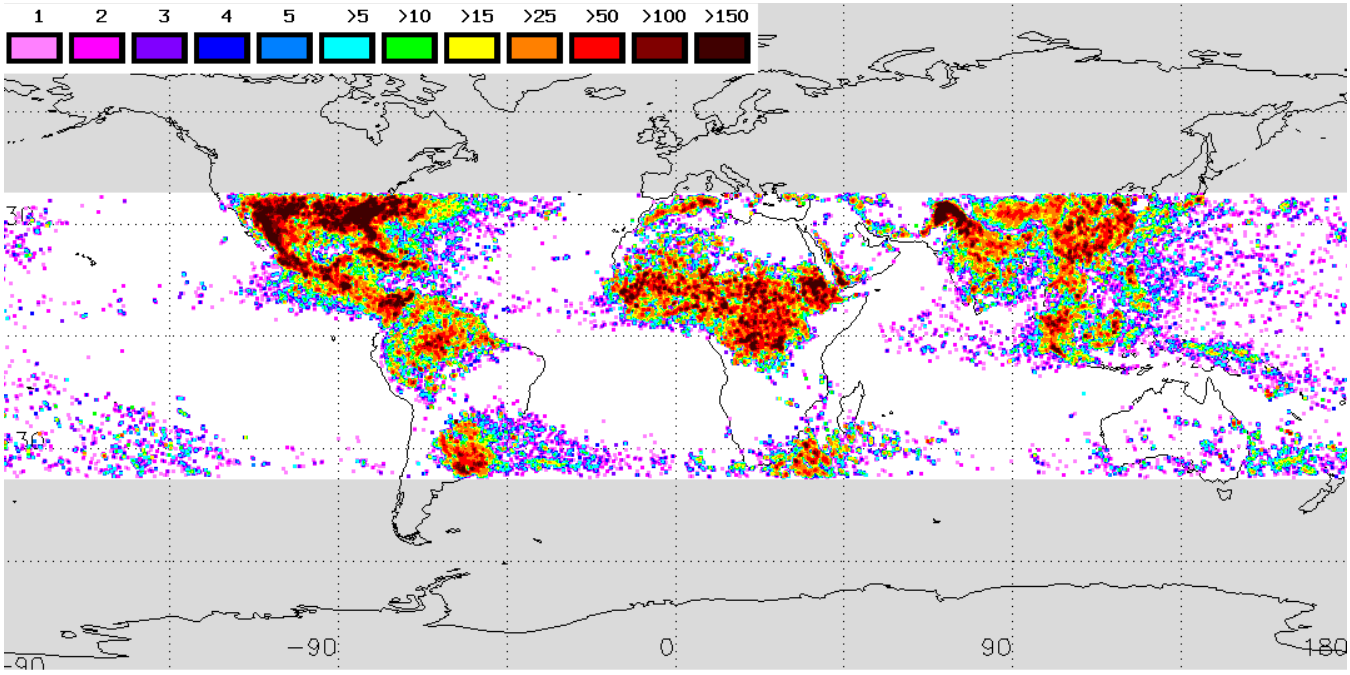

Fig. 9. Lightning distribution in the tropics for winter from LIS data.

bands in winter presented observed period between 10 and 20 minutes.

14. The ripples displayed the same distribution for the observed periods for the four seasons.
15. The observed phase velocity of the bands in winter and summer were of same order, between 10 and 40 m/s.
16. The ripples did not display a clear seasonal variation for observed phase velocity.
17. The ripples did not display clear seasonal variation for propagation direction.
18. The bands displayed an anisotropy in propagation direction. In summer, most of waves propagated for south-

east. In winter, the propagation direction was for northwest.

19. The gravity waves over CP are generated by strong convective regions. In summer, these regions extend over a line from approximately (10° S, 45° W) to (40° S, 78° W), covering from north of Argentina to Brazilian northeast, with an accentuated distribution over central Brazil having CP below this region. In winter, the convective region in contrast to the summer is bellow CP, mainly over the sea and there is no convection in central Brazil region above CP.
20. Finally, maybe the most important conclusion of the work was that the anisotropy of propagation direction is due to partially the location of the generating sources (seasonal variation) and mainly to the wave filtering by stratospheric winds.

BIBLIOGRAPHY

BILLS R. E. and C. S. GARDNER, 1993. Lidar observations of the mesopause region temperature structure at Urbana. *J. Geophys. Res. Atmosph., 98(D1)*, 1011-1021.

BURITI, R. A., 1997. Estudo de parâmetros de ondas de gravidade por medidas simultâneas de radar MU e fotômetro em Shigaraki (35°N,136°L), Japão. São José dos Campos. 176p. (INPE-6647-TDI.624). Phd thesis, Instituto Nacional de Pesquisas Espaciais.

BURNSIDE R. G., C. A. TEPLEY, M. P. SULZER, T. J. FULLER-ROWELL, D. G. TORR and R. G. ROBLE, 1991. The neutral thermosphere at Arecibo during geomagnetic storms, *J. Geophys. Res. Space Phys., 96(NA2),* 1289-1302.

CLAIREMIDI, J., M. HERSE and G. MOREELS, 1985. Bi-dimensional observation of waves near the mesopause at auroral latitudes. *Planet. Space Sci., 33,* 1013-1022.

CLEMESHA, B. R., 1995, Sporadic neutral metal layers in the mesosphere and lower thermosphere. *J. Atmosph. Terr. Phys., 57*, 725-736.

CLEMESHA, B. R., I. VESELOVSKII, P. P. BATISTA, M. P. P. M. JORGE and D. M. SIMONICH, 1999. First mesopause temperature profiles from a fixed southern hemisphere site. *Geophys. Res. Lett., 26(12),* 1681-1684.

FRITTS, D. C. and P. K. RASTOGI, 1985. Convective and dynamical instabilities due to gravity wave motions in the lower and middle atmosphere. Theory and observations. *Radio Science, 20(6),* 1247-1277.

FRITTS, D. C., D. M. RIGGIN, B. B. BALSEY and R. G. STOCKWELL, 1998. Recents results with an MF radar at Mcmurdo, Antartica: Characteristics and variability of motions near 12-hour period in the mesosphere. *Geophys. Res. Lett., 25(3),* 297-300.

GARCIA, F. J. and M. J. TAYLOR, 1997. Two-dimensional spectra-analysis of mesospheric airglow data. *Applied Optics, 36(29),* 7374-7385.

GARDNER, C. S., J. QIAN, M. R. COBLE, G. C. PAPEN and G. R. SWENSON, 1995. High resolution horizontal wave-number spectra of mesospheric wave perturbations observed during the 21 October triangular flight of ALOHA-93. *Geophys. Res. Lett., 22(20),* 2869-2872.

GAULT, W. A., S. BROWN, A. MOISE, D. LIANG, G. SELLAR, G. G. SHEPHERD and J. WIMPERIS, 1996. An E-region wind interferometer. *Applied Optics, 35(16),* 2913-2922.

HAPGOOD, M. A. and M. J. TAYLOR, 1982. Analysis of airglow image data. *Ann. Geophys., 38(6),* 805-813.

HECHT, J. H., S. R. R. HOWAT, R. L. WALTERSCHEID and J. R. ISLER,1995. Observations of spectra of intensity flutuations of the OH Meinel nightglow during ALOHA-93. *Geophys. Res. Lett., 22:(20),* 28373-2876.

HECHT, J. H., R. L. WALTERSCHEID and M. N. ROSS, 1994. First measurements of the two-dimensional horizontal wave number spectrum from CCD images of the nightglow. *J. Geophys. Res. Lett., 99,* 11449-11460.

HECHT, J. H., R. L. WALTERSCHEID, M. P. KICKEY and S. J. FRANKE, 2001. Climatology and modeling of quasi-monochromatic atmospheric gravity waves observed over Urbana Illinois. *J. Geophys. Res., 106,* 5181-5191.

HERNANDES, G., G. J. FRASER and R. W. SMITH, 1993. Mesospheric 12-hour oscillation near south pole, Antarctica. *Geophys. Res. Lett., 20(17),* 1787-1790.

HERSE M., MOREELS G. and J. CLAIREMIDI, 1980. Waves in the OH emissive layer: photogrammetry and topography. *Appl. Optics, 19,* 355-362.

HINES, C. O., 1960. Internal atmospheric gravity waves at ionospheric heights. *Can. J. Phys, 38,* 1441-1481.

ISLER, J. R., M. J. TAYLOR and D. J. FRITTS, 1997. Observational evidence of wave ducting and evanescence in the mesosphere. *J. Geophys. Res., 102,* 26301-26313.

KIRCHENGAST, G., K. HOCKE and K. SCHLEGEL, 1996. The gravity-wave tide relationship - insight via theoretical-model EISCAT data comparison. *J. Atmos. Terr. Phys., 58(1-4),* 233-243.

LOWE, R. P. and D. N. TURNBULL, 1995. Comparison of ALOHA-93, ANLC-93 and ALOHA-90 observations of the hydroxyl rotational temperature and gravity wave activity. *Geophys. Res. Lett., 22(20),* 2813-2816.

MANSON, A. H., C. E. MEEK and Q. M. ZHAN, 1997. Gravity-wave spectra and directions statistics for the mesosphere as observed by MF radars in the canadian Prairies (49°N, 52°W) and at Tromso (69°N). *J. Atmos. Solar Terr. Phys., 59(9),* 993-1009.

MORELS, G. and M. HERSE, 1997. Photographic evidence of waves around the 85 km level. *Planet. Space Science, 25,* 265-273.

NAKAMURA, T., A. HIGASHIKAWA, T. TSUDA and Y. MATSUSHITA, 1999. Seasonal variations of gravity wave structures in OH airglow with a CCD imager at Shigaraki. *Earth Planets Space, 51,* 897-906.

OLIVER, W. L., Y. OTSUKA, M. SATO, T. TAKAMI and S. FUKAO, 1997. A climatology of F-region gravity-wave propagation over middle and upper-atmosphere radar. *J. Geophys. Res. Space Phys., 102(A7),* 14499-14512.

PETERSON, A. W. and L. M. KIEFFABER, 1973. Infrared photography of OH airglow structures. *Nature, 242,* 321-322.

PETERSON, A. W., 1979. Airglow events visible to the naked eye. *Appl. Optics, 22,* 3390-3393.

RIGGIN, D., D. C. FRITTS, C. D. FAWCETT and E. KUDEKI, 1995. Observations of inertial gravity wave motions in the stratosphere over Jicamarca, Peru. *Geophys. Res. Lett., 22(23),* 3239-3242.

RISHBETH, H. and A. P. VANEYKEN, 1993. EISCAT - Early history and the 1st 10 years of operation. *J. Atmosph. Terr. Phys., 55(4-5),* 525-542.

RYAN, E. H., 1991. Critical layer directional filtering of atmospheric gravity waves: A comparison of airglow and wind profile model: M.S. thesis, The Univ. of Cincinnati, Ohio.

RYAN, E. H. and T. F. TUAN, 1991. Gravity waves blocking by critical layers, Middle Atmosphere Periodic Structure and Associated Radiance (MAPSTAR) Meeting, Air Force Geophys. Lab., April.

SHE, C. Y., J. R. YU, J. W. HUANG, C. NAGASAWA and C. S. GARDNER, 1991. Na temperature lidar measurements of gravity wave perturbations of wind, density and temperature in the mesopause region. *Geophys. Res. Lett., 18(7),* 1329-1331.

SHEPHERD, G. G., 1996. WINDII on UARS - a view of upper mesosphere and lower thermosphere dynamics. *J. Geomagnetism and Geoelectricity, 48(1),* 125-133.

SIVJEE, G. G. and R. L. WALTERSHEID, 1994. 6-hour zonally symetrical tidal oscillation of the winter mesopause over the south-pole station. *Planet. Space Sci., 42(6),* 447-453.

SWENSON, G. R. and S. B. MENDE, 1994. Oh emission and gravity waves (including a breaking wave) in all-sky imagery from Bear Lake, UT. *Geophys. Res. Lett., 21,* 2239-2242.

TAKAHASHI, H., P. P. BATISTA, R. A. BURITI, D. GOBBI, T. NAKAMURA, T. TSUDA and S. FUKAO, 1998. Simultaneous measurements of airglow OH emission and meteor wind by a scanning photometer and MU radar. *J. Atmosph. Solar Terr. Phys., 60,* 1649-1668.

TAKAHASHI, H., P. P. BATISTA, R. A. BURITI, D. GOBBI T. NAKAMURA, T. TSUDA and S. FUKAO, 1999. Response of the airglow OH emission, temperature and mesopause wind to the atmospheric wave propagation over Shigaraki, Japan. *Earth Planets Space, 51,* 863-875.

TAKAHASHI, H., B. R. CLEMESHA and Y. SAHAY, 1974. Nightglow OH(8,3) band intensities and rotational temperature at 23 degrees. *Planet. Space Sci., 22,* 1323-1329.

TAYLOR, M. J. and R. EDWARDS, 1991. Observations of short-period mesospheric wave patterns - insitu or tropospheric wave generation. *Geophy. Res. Lett., 18(7),* 1337-1340.

TAYLOR, M. J. and F. J. GARCIA, 1995. A two-dimensional spectral analysis of short period gravity waves

imaged in the OI(557.7 nm) and near infrared OH nightglow emissions over Arecibo, Puerto Rico. *Geophys. Res. Lett., 22,* 2473-2276.

TAYLOR, M. J. and M. A. HAPGOOD, 1990. On the origin of ripple-type wave structure in the nightglow emission. *Planet. Space Sci., 38,* 1421-1430.

TAYLOR, M. J., M. A. HAPGOOD and P. ROTHWELL,1987. Observations of gravity wave propagation in the OI (557.7 nm), Na (589.2 nm) and the near infrared OH nightglow emissions. *Planet. Space Sci, 35,* 413-427.

TAYLOR, M. J. and M. A. HAPGOOD, 1988. Identification of a thunderstorm as a source of short period gravity waves in the upper atmospheric nightglow emissions. *Planet. Space Sci. 36*, 975-985.

TAYLOR, M. J., E. H. RYAN, T. F. TUAN and R. EDWARDS, 1993. Evidence of preferential directions for gravity wave propagation due to wind filtering in the middle atmosphere. *J. Geophys. Res., 98(A4)*, 6047-6057.

THAYAPARAN, T., 1997. The terdiurnal tide in the mesosphere and lower thermosphere over London, Canada (43°N, 81°S). *J. Geophys. Res., 102(D18),* 21695-21708.

VINCENT, R. A. and D. C. FRITTS, 1987. A climatology of gravity wave motions in the mesopause region at Adelaide, Australia. *J. Atmospher. Sci., 44(4),* 748-760.

WALTERSCHEID, R. L., J. H. HECHT, R. A. VICENT, I. M. REID, J. WOITHE and M. P. HICKEY, 1999. Analysis and interpretation of airglow and radar observations of quasi-monochromatic gravity waves in the upper mesosphere and lower thermosphere over Adelaide, Australia (35 S, 138 E). *J. Atmos. Sol. Terr. Phys., 61,* 461-468.

A. F. Medeiros[1], H. Takahashi[2], P. P. Batista[2], D. Gobbi[2] and M. J. Taylor[3]

[1] Universidade Federal Campina Grande (UFCG), Av. Aprígio Veloso 882, Bodocongó, Campina Grande, Paraíba, 58.109-170, Brasil.
[2] Instituto Nacional de Pesquisas Espaciais (INPE), Av. Dos Astronautas 1758, C. Postal: 515, São José dos Campos, São Paulo,12.201-970, Brasil.
[3] Space Dynamics Laboratory and Physics Department, Utah State University, Logan 84322-4145, Utah,USA
Email: afragoso@df.ufpb.br